The 9th European Congress on Computational Methods in Applied Sciences and Engineering
ECCOMAS Congress 2024
3–7 June 2024, Lisboa, Portugal

CONVERGENCE BEHAVIOUR OF PARTITIONED METHODS FOR CONJUGATE HEAT TRANSFER PROBLEMS

VICTOR VAN RIET[1], WIM BEYNE[1], MICHEL DE PAEPE[1,2,3] AND JORIS DEGROOTE[1,2]

[1] Department of Electromechanical, Systems and Metal Engineering, Ghent University
Sint-Pietersnieuwstraat 41, 9000 Ghent, Belgium
e-mail: Victor.VanRiet@UGent.be

[2] FlandersMake@UGent – Core lab MIRO, Ghent, 9000, Belgium

[3] Department of Mechanical Engineering, University of Cape Town
Private Bag X3, Rondebosch 7701, South Africa

Key words: Conjugate heat transfer, Partitioned coupling algorithms, Numerical stability, CFD, Biot number

Summary. Conjugate heat transfer (CHT) considers the simultaneous solution of heat transfer in adjacent solid and fluid domains. If solved with a partitioned approach, temperature and heat flux are exchanged to achieve a thermal equilibrium at the interface. Gauss-Seidel iterations, however, are only stable for a limited range of Biot numbers because temperature and heat flux are exchanged unmodified. In order to extend the stability range of Gauss-Seidel iterations, static relaxation, Aitken relaxation or quasi-Newton methods can be used. These methods are tested on a heated flat plate problem, both in steady state and transient simulations, and their convergence behaviour is analysed. Using temperature as input for the fluid solver and heat flux as input for the solid solver converges best for steady state simulations, while the opposite is most stable for transient cases. Furthermore, the quasi-Newton method converges slightly better than the relaxation methods in transient simulations with rapid changes at the interface.

1 INTRODUCTION

Conjugate heat transfer (CHT) considers the simultaneous solution of heat transfer in adjacent solid and fluid domains. CHT problems have a widespread occurrence in many engineering fields, with applications such as internally-cooled turbine blades [1], thermal storage [2] and cooling of electronics [3]. A thorough review of the applied and theoretical aspects of CHT analysis is provided by [4].

In conjugate heat transfer problems, the conductive heat transfer equation is solved in the solid domain and the energy equation containing a convection term in the fluid domain, together with the flow equations. In such a fluid-thermal interaction (FTI) problem, the solid and liquid domains are coupled by a single interface temperature and heat flux, with the heat flux opposite in sign between both domains. This coupled system of equations can be solved together, which is called the monolithic approach, or separately for each domain, which is the partitioned approach.

The partitioned approach requires iterations between the solvers of the solid and fluid domains to satisfy the interface conditions. This has the advantage that existing and optimised solvers can be used for both solid and fluid. The coupling iterations, however, can be unstable and computationally expensive [8].

Clearly, FTI's problem statement is very similar to that of fluid-structure interaction (FSI). Instead of thermal interaction between a solid and a fluid, FSI comprises the kinematic and dynamic interaction between a fluid and a moving or deforming solid structure [9]. In FTI as well, the coupled problem can be solved in a monolithic or partitioned way. In the partitioned approach, strongly coupled FSI problems require coupling iterations between the fluid and structure solver to reach equilibrium of displacement and traction at the interface. This is equivalent to the coupling iterations needed achieve continuity of temperature and heat flux on the interface of an FTI problem.

Depending on the physics of the problem, straightforward fixed-point iterations between fluid and solid solver can lead to instabilities or slow convergence for both FSI and FTI problems, if no additional stabilisation measures are applied. For FSI, high added mass of the system makes the iterations less stable [9]. Added mass is the effective increase in an object's inertia due to fluid displacement during motion. In the case of FTI, the stability depends largely on the Biot number Bi of the problem, which is the ratio of the conductive thermal resistance of the solid to the convective resistance of the fluid [8].

For conjugate heat transfer, most common coupling techniques are based on the choice of boundary condition and relaxation of the input for each solver. Both the solid and fluid domains can have a temperature (Dirichlet) or heat flux (Neumann) boundary condition, with one domain's boundary condition naturally the opposite of the other's. Robin boundary conditions, in which a virtual heat transfer coefficient is passed between the domains, are also among the possibilities [8]. In FSI, fixed-point iterations with relaxation can be employed as well, but more advanced techniques, such as Aitken relaxation [11], and especially quasi-Newton methods have been found to improve convergence speed drastically for strongly coupled problems [10].

Quasi-Newton methods have already been successfully used to solve FTI problems [5, 6], but their stabilisation performance was never compared to simpler alternatives such as relaxation on the same case. In this study, CHT capabilities have been added to the partitioned coupling tool for FSI *CoCoNuT*. As such, Aitken and quasi-Newton methods, originally implemented for FSI problems, can be used for the thermal coupling in CHT problems as well. This way, the convergence behaviour of these advanced coupling techniques can be studied when applied to CHT problems and their performance can be compared to (relaxed) Gauss-Seidel iterations.

In the next section, the different coupling methods are explained. These will be tested on a heated flat plate test case, which is introduced in section 3. Lastly, section 4 presents the convergence analysis and compares the performance of the different coupling methods.

2 COUPLING METHODS

During Gauss-Seidel iterations, the solid and fluid domains are solved successively with exchange of interface data between the two. In this paper, we constrict the definition of the Gauss-Seidel method to iterations where the output of one solver is directly used as input of the other solver. By modifying the output before it is given as an input to the other solver, the Gauss-Seidel iterations can be stabilised. This section presents the different coupling methods

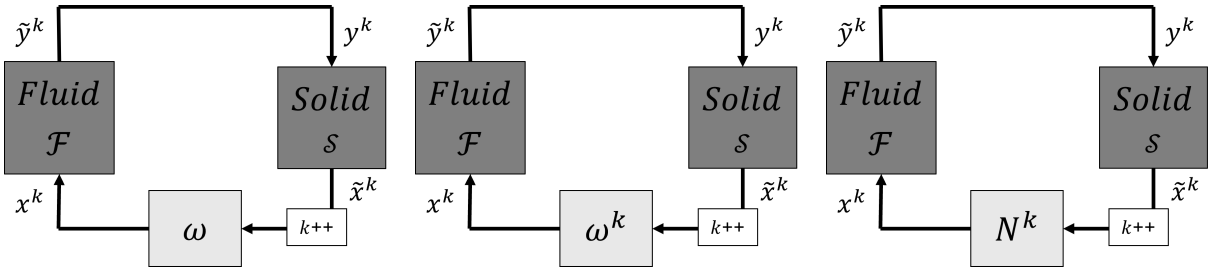

(a) Gauss-Seidel method with fixed relaxation (b) Aitken relaxation method (c) Residual quasi-Newton method

Figure 1: Schematic representation of iteration methods

studied in this paper and how they modify the input of the solvers. A summary can be found in Figure 1.

2.1 Gauss-Seidel method

Gauss-Seidel iterations are the simplest way to iterate between the fluid and solid solver. The output of one solver is directly passed on to the second solver without modification until convergence is reached, meaning that the output of the solvers in two successive iterations has no significant difference [10]. In CHT, both temperature T and heat flux q along the interface can be passed between solvers. Which solver receives and returns which variable defines two different Gauss-Seidel schemes for CHT: Flux Forward Temperature Back (FFTB) scheme and Temperature Forward Flux Back (TFFB) scheme [8].

The naming convention was introduced by [12] and defines the schemes after the variables transferred relative to the fluid domain. For FFTB, the interface temperature distribution is passed on to the fluid solver, which returns the resulting heat flux distribution as output to the solid solver. This is schematically shown in Figure 2a. For TFFB, the variable exchange is reversed, which means that the interface heat flux distribution is passed on to the fluid solver, and the interface temperature distribution is returned to the solid solver, as shown in Figure 2b. Both temperature and heat flux are scalar fields at the interface because the exchanged heat flux is the magnitude of the component normal to the interface, being negative in case heat leaves the domain, and positive in case heat enters.

(a) Flux Forward Temperature Back (b) Temperature Forward Flux Back

Figure 2: Two ways of exchanging variables between the fluid and solid domain

Figure 1a shows a general schematic representation of the pure Gauss-Seidel method in case no relaxation ($\omega = 1$) is applied. In the figure, vector $\boldsymbol{x} \in \mathbb{R}^{n\times 1}$ represents the vector passed from solid solver to fluid solver, and $\boldsymbol{y} \in \mathbb{R}^{n\times 1}$ represents the vector passed from fluid to solid

solver. n denotes the number of faces on the discretised interface, assuming the fluid and solid domain have matching cell faces at the interface, which is the case in this study. n is also the length of both $\boldsymbol{x}$ and $\boldsymbol{y}$ because temperature and heat flux are scalar fields. The variables associated with $\boldsymbol{x}$ and $\boldsymbol{y}$ change whether the FFTB or TFFB scheme is used. As a result, for FFTB, Eq. 1 applies, and for TFFB, Eq. 2 is valid.

$$\begin{aligned} \boldsymbol{x} &= \begin{bmatrix} T_1 & T_2 & \dots & T_n \end{bmatrix}^T \\ \boldsymbol{y} &= \begin{bmatrix} q_1 & q_2 & \dots & q_n \end{bmatrix}^T \end{aligned} \tag{1}$$

$$\begin{aligned} \boldsymbol{x} &= \begin{bmatrix} q_1 & q_2 & \dots & q_n \end{bmatrix}^T \\ \boldsymbol{y} &= \begin{bmatrix} T_1 & T_2 & \dots & T_n \end{bmatrix}^T \end{aligned} \tag{2}$$

In the remainder of this section, the $\boldsymbol{x}$ and $\boldsymbol{y}$ notation will be used. As such, the remaining coupling methods can be used with both the FFTB and TFFB scheme. The flow solver is denoted as $\mathcal{F}(\boldsymbol{x})$ with input $\boldsymbol{x}$ and the solid solver is $\mathcal{S}(\boldsymbol{y})$ with input $\boldsymbol{y}$. The output of the solvers is denoted with a tilde, resulting in

$$\begin{aligned} \tilde{\boldsymbol{y}}^k &= \mathcal{F}\left(\boldsymbol{x}^k\right) \\ \tilde{\boldsymbol{x}}^k &= \mathcal{S}\left(\boldsymbol{y}^k\right) \end{aligned} \tag{3}$$

for iteration k. While the set of equations above holds for every coupling method introduced in this paper, the difference lies in how the output of one solver translates to the input of the other solver. In case of Gauss-Seidel iterations, the variables are passed on unchanged:

$$\begin{aligned} \boldsymbol{y}^k &= \tilde{\boldsymbol{y}}^k \\ \boldsymbol{x}^{k+1} &= \tilde{\boldsymbol{x}}^k \end{aligned} \tag{4}$$

For the other coupling techniques discussed in this paper, $\boldsymbol{y}$ will always be imposed from fluid to solid solver unchanged. Solid solver output $\tilde{\boldsymbol{x}}^k$, however, will be modified before being used as input for the fluid solver in an attempt to stabilise the iterations. These modifications will be discussed in the following subsections.

2.2 Fixed relaxation method

The simplest way to stabilise the coupling iterations is to mix the new and old input by using a fixed relaxation factor ω, which takes a value between 0 and 1. This depicted in Figure 1a.

$$\boldsymbol{x}^{k+1} = (1-\omega)\boldsymbol{x}^k + \omega\tilde{\boldsymbol{x}}^k \tag{5}$$

Verstraete and Scholl [8] analytically derived guidelines on how to choose relaxation factors based on a 1D conjugate heat transfer problem. The stability was shown to depend on the local Biot number Bi. The Biot number is defined as $Bi = \frac{hL}{\lambda_s}$, in which h is the heat transfer coefficient at the fluid side, L is the characteristic length and λ_s is the solid conduction coefficient. As such, Bi represents the ratio of the thermal resistance in the solid domain over the fluid domain. Verstraete and Scholl found that the FFTB method only converges for $|Bi| < 1$ and

the TFFB method only for $|Bi| > 1$. The range of stable Biot numbers can be extended by relaxation. Depending on Bi, the relaxation factor should be chosen as

$$\begin{aligned} \omega &< \frac{2}{Bi+1} \quad \text{, for FFTB} \\ \omega &< \frac{2Bi}{Bi+1} \quad \text{, for TFFB} \end{aligned} \tag{6}$$

Using the equations above, the FFTB method can be stabilised based on the highest numerical value of Bi and the TFFB method on the lowest numerical value of Bi. Some fine-tuning might be needed, but Eq. 6 can provide a first estimate for ω.

A relaxation factor closer to zero stabilises the iterations more but slows down convergence. Often, the relaxation factor is determined by the least stable part of the coupling iterations. As such, ω is suboptimal for a large part of the simulation, which increases the total calculation time unnecessarily. This can be avoided by using a dynamic relaxation factor, as with Aitken relaxation.

2.3 Aitken relaxation method

Aitken relaxation [11] applies a dynamic relaxation coefficient ω^k, which is updated every iteration. As shown in Figure 1b, ω^k is used in the same way as ω in static relaxation:

$$\boldsymbol{x}^{k+1} = (1-\omega^k)\boldsymbol{x}^k + \omega^k \tilde{\boldsymbol{x}}^k \tag{7}$$

The value of ω^k is obtained as

$$\omega^k = \omega^{k-1} \frac{-\left(\mathbf{r}^{k-1}\right)^T \left(\mathbf{r}^k - \mathbf{r}^{k-1}\right)}{\left(\mathbf{r}^k - \mathbf{r}^{k-1}\right)^T \left(\mathbf{r}^k - \mathbf{r}^{k-1}\right)} \tag{8}$$

which can be interpreted as the secant method for scalars applied directly to vectors and projecting it on $\mathbf{r}^k - \mathbf{r}^{k-1}$. $\mathbf{r}^k$ is the residual, which is defined as $\tilde{\boldsymbol{x}}^k - \boldsymbol{x}^k$. The first relaxation factor ω^0 in a time step is taken equal to the last relaxation factor from the previous time step ω^n, but limited to a maximal value ω^{max}.

2.4 Quasi-Newton method

Quasi-Newton methods go a step further than a scalar dynamic relaxation factor. They can be interpreted as using dynamic relaxation factors, not only per iteration, but for different Fourier modes of the output of the second solver $\tilde{\boldsymbol{x}}$ as well. The quasi-Newton method used in this study is the IQN-ILS method, meaning interface quasi-Newton with the inverse Jacobian approximated from a least-squares model.

The fluid solver $\mathcal{F}$ and the solid solver $\mathcal{S}$, as shown in Figure 1c, are combined into a single system with input $\boldsymbol{x}^k$ and output $\tilde{\boldsymbol{x}}^k$ in the k^{th} iteration. This can be written as

$$\tilde{\boldsymbol{x}}^k = \mathcal{S} \circ \mathcal{F}\left(\boldsymbol{x}^k\right) \tag{9}$$

with $\circ$ denoting function composition. As defined in section 2.3, the difference between output and input is the residual $\mathbf{r}^k = \tilde{\boldsymbol{x}}^k - \boldsymbol{x}^k$. Based on Eq. 9, the residual can be expressed as the output of the residual operator $\mathcal{R}(\boldsymbol{x})$:

$$\mathcal{R}\left(\boldsymbol{x}^k\right) = \mathcal{S} \circ \mathcal{F}\left(\boldsymbol{x}^k\right) - \boldsymbol{x}^k = \mathbf{r}^k \tag{10}$$

As such, the coupled problem can be reduced to Eq. 11.

$$\mathcal{R}\left(\boldsymbol{x}\right) = 0 \tag{11}$$

This set of nonlinear equations can be solved in $\boldsymbol{x}$ by Newton-Raphson iterations:

$$\Delta\boldsymbol{x}^k = \mathcal{R}'^{-1}\left(\boldsymbol{x}^k\right)\Delta\mathbf{r}^k \tag{12}$$

where $\mathcal{R}'^{-1}$ represents the inverse Jacobian of $\mathcal{R}$, $\Delta\boldsymbol{x}^k = \boldsymbol{x}^{k+1} - \boldsymbol{x}^k$ is the difference between the input of two successive iterations and $\Delta\mathbf{r}^k = 0 - \mathbf{r}^k$ is the difference between the zero residual and the current residual. As such, the new input $\boldsymbol{x}^{k+1}$ is chosen with the aim to bring the residual to zero.

The solvers, however, are perceived as a black-box and the Jacobian $\mathcal{R}$ is not accessible. As a result, an approximation $\boldsymbol{N}^k$ must be constructed for $\mathcal{R}'^{-1}\left(\boldsymbol{x}^k\right)$. The Newton-Raphson iterations require $\boldsymbol{N}^k$ to be full rank to function properly, whereas the approximation procedure typically produces a low-rank estimate Jacobian. Consequently, the inverse Jacobian is approximated not for $\mathcal{R}$, but for an altered residual operator $\widetilde{\mathcal{R}}$, which is defined below.

$$\mathbf{r}^k = \widetilde{\mathcal{R}}\left(\tilde{\boldsymbol{x}}^k\right) = \mathcal{R}\left(\tilde{\boldsymbol{x}}^k - \mathbf{r}^k\right) \tag{13}$$

The inverse of both Jacobian formulations are linked by

$$\widetilde{\mathcal{R}}'^{-1} = \mathcal{R}'^{-1} + \boldsymbol{I} \tag{14}$$

Using $\widetilde{\mathcal{R}}$, the Newton-Raphson iteration of Eq. 12 can be rewritten as

$$\Delta\tilde{\boldsymbol{x}}^k = \widetilde{\mathcal{R}}'^{-1}\left(\boldsymbol{x}^k\right)\Delta\mathbf{r}^k \tag{15}$$

with $\Delta\tilde{\boldsymbol{x}}^k$ defined as $\tilde{\boldsymbol{x}}^{k+1} - \tilde{\boldsymbol{x}}^k$. The Jacobian $\widetilde{\mathcal{R}}'^{-1}\left(\boldsymbol{x}^k\right)$ is also not accessible, but is better suited to be estimated. The approximated Jacobian is denoted as $\widetilde{\boldsymbol{N}}^k$. The model used to estimate the inverse Jacobian is the least-squares model. For more details on this model, the reader is referred to [10].

3 TEST CASE: HEATED FLAT PLATE

All three coupling methods (relaxation, Aitken and quasi-Newton) can be used with both the FFTB and TFFB scheme, resulting in a total of 6 methods. These will be tested on a simple but challenging validation case: the heated flat plate. The performance of the methods will be evaluated in both steady state and transient cases.

3.1 Problem definition

The heated flat plate is selected as test case because it allows a wide Bi range at the interface, despite its conceptual simplicity. As such, all methods can be tested at their stability limits. Furthermore, the analytical solution by Luikov [7] allows to benchmark the numerical solution. The geometry and boundary conditions are shown in Figure 3.

The dimensions and boundary conditions are inspired by the work of Verstraete and Scholl [8]. The plate has a thickness b of 0.01 m and a length L of 0.20 m. The bottom of the plate has

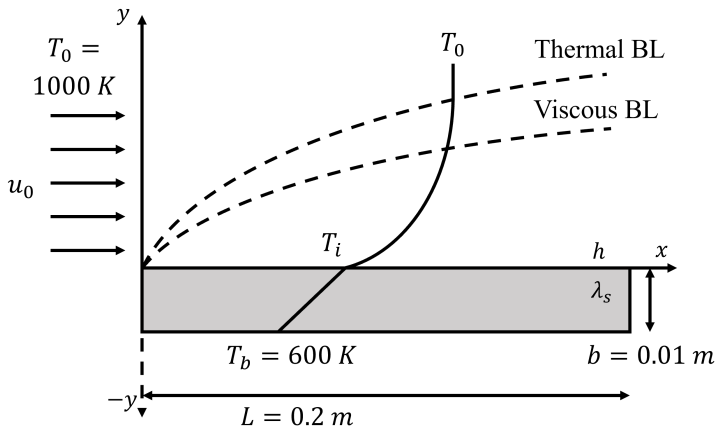

Figure 3: Geometry and boundary conditions of the flat plate solid and fluid domain allowing numerical Bi values to vary between 0.25 and 35 depending on inlet velocity u_0

a fixed temperature boundary condition T_b of 600 K and is heated from the top by a parallel flow. The flow has a uniform inlet velocity u_0 and temperature T_0. Consequently, a viscous and thermal boundary layer will develop starting from the tip of the plate. The uniform inlet temperature T_0 will remain fixed for all cases at 1000 K, while u_0 will be changed throughout the different cases. A uniform static pressure of $1.03 \cdot 10^5$ Pa is maintained at the outlet. The fluid is air, which is modelled as incompressible with properties at 1000 K as defined in Table 1. The conduction coefficient of the solid λ_s is set equal to 0.2876 W/mK.

Table 1: Properties of air at 1000 K and $1.03 \cdot 10^5$ Pa, based on [8]

Property	Value	Unit
ρ	0.3525	kg/m^3
c_p	1142.6	J/kgK
μ	$3.95 \cdot 10^{-5}$	kg/ms
λ_f	0.06808	W/mK

For all tested cases, the material properties ensure laminar flow. In that case, the following analytical solution for the local Biot number by Luikov [7] is valid.

$$Bi_x = 0.332 \cdot b \frac{\lambda_f}{\lambda_s} Pr^{1/3} \frac{Re_x^{1/2}}{x} \tag{16}$$

Figure 4 shows the Biot number distribution across the solid-fluid interface according to Eq. 16 for four different values of inlet velocity. As the inlet velocity increases, the convection at the fluid side becomes more effective, which increases Bi along the entire interface length. For all velocities, however, there exist both regions at the interface with $Bi > 1$ and $Bi < 1$. For increasing velocity, the point at which $Bi = 1$ shifts to the right on the interface because of the upwards moving curve.

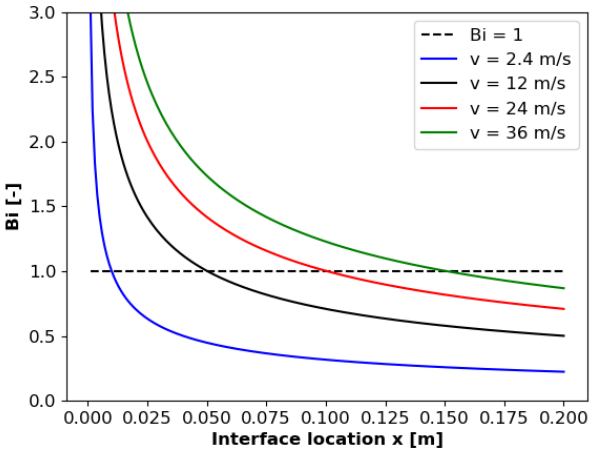

Figure 4: Analytical Biot number as a function of x coordinate on the solid-fluid interface

By ensuring that the local Bi is both larger and smaller than 1 for specific regions of the interface, the FFTB scheme, as well as the TFFB scheme, will be challenged in all cases presented below. As the regions for $Bi < 1$ or $Bi > 1$ become larger or smaller, both coupling schemes will become more or less suited for the problem at hand. This allows to study their stability and convergence behaviour. Based on the analytical study by Verstraete and Scholl [8], the FFTB scheme is expected to perform better for cases with low average Bi, and the TFFB scheme for high average Bi cases.

3.2 Solvers

The finite volume solver Fluent 2023R1 was used for both the fluid and solid domain. Different settings were used, however. In the solid domain, only the energy equation, which is discretised with a 2^{nd} order upwind scheme, is considered. The fluid solver is a pressure-based solver which employs a 2^{nd} order upwind scheme too for the discretisation of both the energy and momentum equation. Velocity and pressure are solved in a coupled fashion for the steady state cases and the SIMPLE algorithm is used for the transient cases. In the transient cases, a 2^{nd} order implicit scheme is used for time stepping in both fluid and solid domains with a time step size of 0.01 s.

3.3 Grid

The solid domain takes the dimensions of the plate, which is 0.2 m in length and 0.01 m in height. The fluid domain is divided in two parts: a main section directly above the flat plate and an inlet section in front of the main section. The main section is 0.2 m in length as well as in height, while the inlet section is 0.1 m in length and 0.2 m in height.

The grids are based on the ones presented in Verstraete and Scholl [8], who performed a grid independence study. Due to the use of finite volume solvers in the present study, the conclusions drawn from their grid study employing finite element solvers cannot be directly extrapolated. As a result, the grid independence study was repeated and the same resolution as in [8] proved sufficient for grid convergence of temperature and heat flux at the interface.

Both the solid and fluid domain have a structured grid with matching cell faces at the interface to avoid the need for interpolation between both grids. The selected solid grid has 80 by 30

cells and the selected fluid grid has 80 by 100 cells for the main section and 40 by 100 for the inlet section. This results in a cell count of 2400 cells for the solid grid and 12000 cells for the combined fluid grid.

4 STABILITY ANALYSIS

4.1 Steady state test case

The steady state simulations are performed with four uniform inlet velocities: 2.4 m/s, 12 m/s, 24 m/s and 36 m/s. The Bi distribution at the interface according to the analytical solution of Luikov [7] is shown in Figure 4 for the different velocities. As can be seen, the curve shifts upward for increasing velocity because of the increase in average Bi. The velocities have been chosen in such a way that $Bi = 1$ at respectively $x = 0.01$ m, 0.05 m, 0.10 m and 0.15 m. As such, the FFTB schemes will be challenged more at higher inlet velocities, because $Bi > 1$ for a larger part of the interface and vice versa for the TFFB schemes.

For the fixed relaxation method, adequate relaxation factors ω should be chosen depending on the inlet velocity and the iteration scheme (FFTB or TFFB) according to Eq. 6. After fine-tuning, the relaxation factors for the FFTB scheme are 0.48, 0.32, 0.22 and 0.2 listed for increasing velocity. Similarly, for the TFFB scheme, the relaxation factors are 0.4, 0.65, 0.75 and 0.75 listed for increasing velocity.

The convergence is quantified by the number of coupling iterations needed for convergence. The convergence criterion is applied to the 2^{nd} order norm of the residual of the temperature distribution at the interface. Convergence is fulfilled when the absolute norm or relative norm is smaller than respectively 10^{-2} K or 10^{-2}. Figure 5 shows the necessary coupling iterations for each method and for all four velocities.

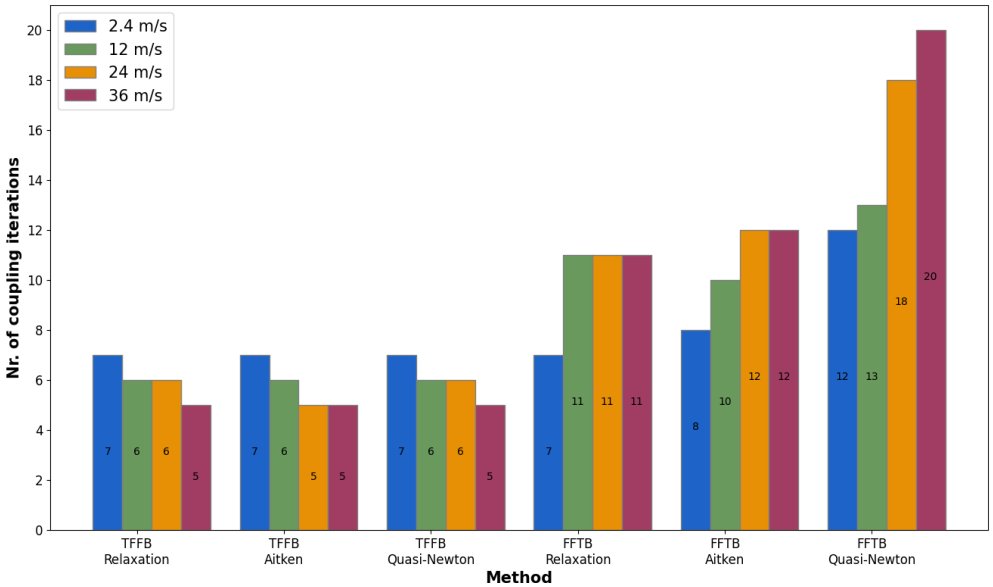

Figure 5: Number of coupling iterations needed for convergence for each method and each inlet velocity for the steady state cases

As can be seen, the TFFB scheme performs better than the FFTB scheme for every method

used in the steady state cases, except for the relaxation methods at the lowest inlet velocity where they perform similarly. This might be explained by the Bi peak at the leading edge of the plate, as can be seen in Figure 4. The asymptotic approach at the tip is harder to converge to than the gradual decline of Bi at the trailing edge, starting from a constant temperature initial interface condition at 800 K. This favours the TFFB scheme, which is more stable at high Bi.

Between the different methods using the TFFB scheme, there is no significant difference in performance despite the increased complexity of the Aitken method and especially the quasi-Newton method. Even more so, the quasi-Newton method performs significantly worse than the relaxation and Aitken method using the FFTB scheme. The number of coupling iterations necessary to build the approximate Jacobian hinders convergence for the quasi-Newton method in the steady state case.

4.2 Transient test case

For the transient test cases, a time-variable inlet velocity is applied, which is still uniform over the full length of the inlet. The four velocity profiles are shown in Figure 6 as a function of time. The velocity will either sinusoidally increase from 2.4 m/s to 36 m/s in a given time span and remain fixed at 36 m/s for the same time span, or sinusoidally decrease from 36 m/s to 2.4 m/s and remain fixed at 2.4 m/s. For both the increasing and decreasing velocity profile, a slow and fast velocity change will be tested. The slow transient changes the velocity in a time span of 10 s and remains fixed at the final velocity for another 10 s, while the fast transient does the velocity change in 1 s and remains at constant velocity for an additional 1 s.

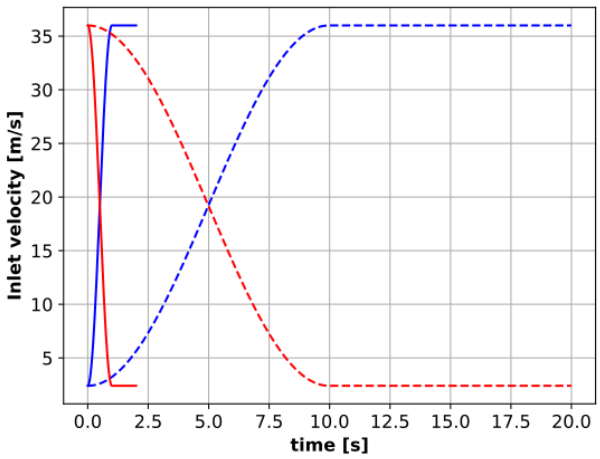

Figure 6: Transient profiles of 4 uniform inlet velocities for the transient cases

Because all velocity profiles have an equal velocity range, the same relaxation factors are chosen: $\omega = 0.2$ for the FFTB scheme and $\omega = 0.05$ for the TFFB scheme. Furthermore, in transient cases, the least-squares technique used for estimating the Jacobian includes information from previous time steps. Considering the 3 most recent time steps yielded the best results in our parameter analysis. Using these parameters, the number of coupling iterations necessary for convergence, averaged over all time steps, is shown in Figure 7. The same convergence criteria as in the steady state cases are used.

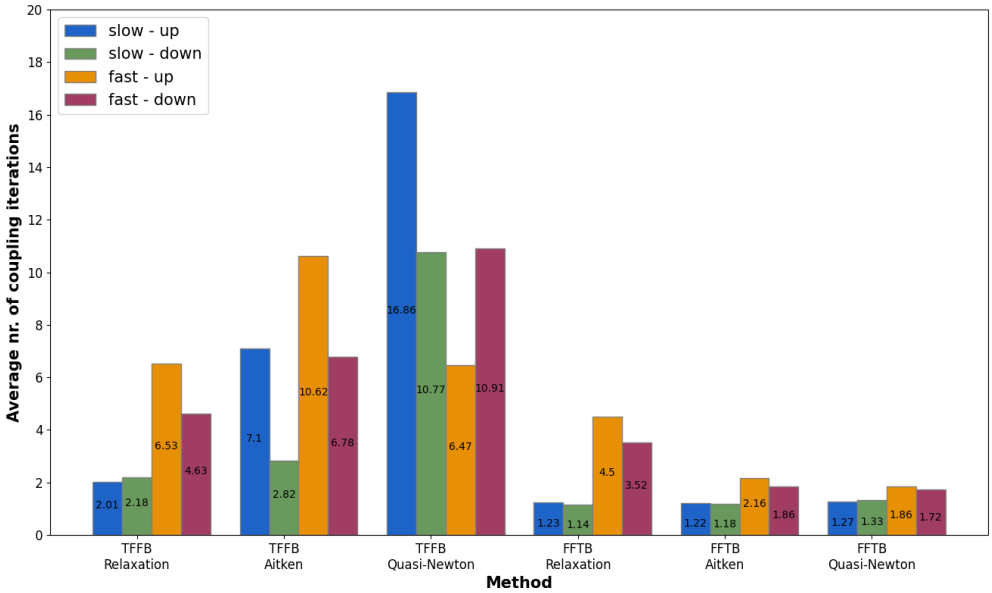

Figure 7: Average number of coupling iterations needed for convergence for each method and each inlet velocity profile for the transient cases

For the transient cases, the FFTB scheme performs better than the TFFB scheme for all methods and all velocity profiles. This behaviour is opposite to the steady state cases, where the TFFB scheme performed best. For transient simulations starting from converged interface conditions, which is the case in this study, this convergence behaviour corresponds to the analytically derived stability analysis by Giles [14]. Giles concluded that the FFTB scheme is more stable because the heat capacity of the computational cell at the fluid side is much lower than heat capacity at the solid side of the interface.

Using the FFTB scheme, the three methods perform similar for the slow transients, and the quasi-Newton method performs best for the fast transients. With the TFFB scheme, the relaxation method performs best for the slow transient cases while the quasi-Newton method converges very slowly. The fast transient cases give a mixed result using the TFFB scheme. The quasi-Newton method performs best for increasing velocity, although relaxation is very close, but performs the worst for the decreasing velocity. It is clear that the fast transient cases challenge the coupling methods more because the interface conditions change more between time steps. Using the FFTB scheme, which seems more suiting for transient problems, more advanced methods (Aitken and quasi-Newton) are able to provide faster convergence.

5 CONCLUSION

Conjugate heat transfer capabilities have been implemented in the FSI coupling tool *CoCoNuT* by enabling exchange of temperature- and heat flux boundary conditions between solid and fluid solvers. Depending on the Biot number at the interface, unrelaxed Gauss-Seidel iterations do not converge and stabilisation methods need to be used. This study tests the performance of three methods, originally implemented for fluid-solid coupling in FSI problems, for stabilising coupling iterations in conjugate heat transfer problems. These methods, being relax-

ation, Aitken relaxation and the quasi-Newton method, are tested on a heated flat plate problem in both steady state and transient problems. This shows that the order in which temperature and heat flux are exchanged is particularly important. Temperature Forward Flux Back schemes perform best in steady state cases, while Flux Forward Temperature Back schemes perform best in transient cases. Furthermore, the quasi-Newton method only converges faster in fast transient problems, while it performs significantly worse in steady state or slow transient cases.

REFERENCES

[1] Scholl, S., Verstraete, T., Duchaine, F. and Gicquel, L. 2016. "Conjugate heat transfer of a rib-roughened internal turbine blade cooling channel using large eddy simulation." Int. J. Heat Fluid Flow 61, 650-664.

[2] Kurnia, J. C., Sasmito, A. P., Jangam, S. v. and Mujumdar, A. S. 2013. "Improved design for heat transfer performance of a novel phase change material (PCM) thermal energy storage (TES)." Appl. Therm. Eng., 50(1), 896–907.

[3] Bondareva, N. S. and Sheremet, M. A. 2018. "Conjugate heat transfer in the PCM-based heat storage system with finned copper profile: Application in electronics cooling." Int. J. Heat Mass Transfer, 124, 1275–1284.

[4] John, B., Senthilkumar, P. and Sadasivan, S. 2019. "Applied and Theoretical Aspects of Conjugate Heat Transfer Analysis: A Review." Arch. Comput. Methods Eng. 26(2), 475–489.

[5] Rüth, B., Uekermann, B., Mehl, M., Birken, P., Monge, A. and Bungartz, H. J. 2021. "Quasi-Newton waveform iteration for partitioned surface-coupled multiphysics applications." Int. J. Numer. Methods Eng. 122(19), 5236–5257.

[6] Mayeli, P. and Nikfar, M. 2019. "Temperature identification of a heat source in conjugate heat transfer problems via an inverse analysis." Int. J. Numer. Methods Heat Fluid Flow. 29(10), 3994–4010.

[7] Luikov, A. v. 1974. "Conjugate convective heat transfer problems." Int. J. Heat Mass Transfer, 17(2), 257–265.

[8] Verstraete, T. and Scholl, S. 2016. "Stability analysis of partitioned methods for predicting conjugate heat transfer." Int. J. Heat Mass Transfer, 101, 852–869.

[9] Delaissé, N., Demeester, T., Haelterman, R. and Degroote, J. 2023. "Quasi-Newton Methods for Partitioned Simulation of Fluid–Structure Interaction Reviewed in the Generalized Broyden Framework." Arch. Comput. Methods Eng. , 30(5), 3271–3300.

[10] Delaissé, N., Demeester, T., Fauconnier, D. and Degroote, J. 2021. "Comparison of different quasi-Newton techniques for coupling of black box solvers." ECCOMAS 2020, Proc., 12.

[11] Küttler, U. and Wall, W. A. 2008. "Fixed-point fluid-structure interaction solvers with dynamic relaxation." Comput. Mech., 43(1), 61–72.

[12] Divo, E., Steinthorsson, E., Rodriquez, F., Kassab, A. J., Kapat, J. S. and Heidmann, J. D. 2003. "Glenn-ht/bem Conjugate Heat Transfer Solver for Large-scale Turbomachinery Models." NASA, Glenn Research Center.

[13] Richardson, L. F. and Gaunt, J. A. 1927. "The deferred approach to the limit." Philos. Trans. R. Soc. London, Ser. A, 226(636–646), 299–361.

[14] Giles, M. B. 1997. "Stability analysis of numerical interface conditions in fluid-structure thermal analysis." Int. J. Numer. Methods Fluids, 25, 421–436.